

Characterization of hydrogen absorption/desorption states on lithium-carbon-hydrogen system by neutron diffraction

Hiroki Miyaoka,¹ Keiji Itoh,² Toshiharu Fukunaga,² Takayuki Ichikawa,^{3,a)} Yoshitsugu Kojima,³ and Hironobu Fuji³

¹Department of Quantum Matter, ADSM, Hiroshima University, 1-3-1 Kagamiyama, Higashi-Hiroshima 739-8530, Japan

²Research Reactor Institute, Kyoto University, Kumatori-cho, Sennan-gun, Osaka 590-0494, Japan

³Institute for Advanced Materials Research, Hiroshima University, 1-3-1 Kagamiyama, Higashi-Hiroshima 739-8530, Japan

(Received 13 January 2008; accepted 10 May 2008; published online 10 September 2008)

The nanostructural hydrogenated graphite ($C^{\text{nano}}H_x$) was synthesized from graphite by ball milling under hydrogen (H_2) atmosphere. In this product, characteristic hydrogenated states in the form of polarized hydrocarbon groups ($-CH$, $-CH_2$, and $-CH_3$) are realized in the nanoscale. By synthesizing the composite of $C^{\text{nano}}H_x$ and lithium hydride (LiH), known as the Li—C—H system, hydrogen was desorbed at 350 °C, which is a lower temperature compared to the decomposition temperature of each component. It is considered that this hydrogen desorption would be induced by destabilization of each hydrogen absorbed state due to an interaction between the polarized C—H groups in $C^{\text{nano}}H_x$ and LiH. Therefore, in order to understand the hydrogen absorption/desorption mechanism of the Li—C—H system, it is an important issue to investigate the change in the C—H groups during hydrogen absorption/desorption reactions in the composite. The correlations among atoms contained in this composite are examined by neutron diffraction measurements, where the protium/deuterium (H/D) isotopic substitution was used to clarify the location of hydrogen atoms in this composite. Some C—D and Li—D correlations are found from the radial distribution function [RDF(r)] obtained by the neutron diffraction for the $C^{\text{nano}}D_x$ and LiD composite. After dehydrogenation, C—C triple bond and Li—C bond, ascribed to lithium carbide (Li_2C_2), are observed. Furthermore, the RDF(r) corresponding to rehydrogenated composite indicates the presence of not only the Li—D correlation but also the C—D one. © 2008 American Institute of Physics. [DOI: 10.1063/1.2956504]

I. INTRODUCTION

Recently, hydrogen storage materials received much attention because it is expected that these materials possess potential application as a suitable energy carrier to establish a clean and sustainable society. On the basis of such a background, materials based on various light elements are being researched all over the world for on-board application,¹⁻³ which would realize gravimetrically and volumetrically high densities of hydrogen. Among them, a lot of carbon based materials have been investigated since Dillon *et al.* reported on single-walled carbon nanotubes as a hydrogen storage material in 1997.⁴ In particular, we have focused on nanostructural hydrogenated graphite ($C^{\text{nano}}H_x$) and have investigated the hydrogen absorption/desorption properties.⁵⁻⁹ The $C^{\text{nano}}H_x$ product was synthesized from graphite by mechanical ball milling under hydrogen atmosphere for 80 h. During the ball-milling process, it is expected that a large amount of active edges or defects is generated in graphene sheets because the graphite structure has been broken down to several nanometer size. Therefore, hydrogen atoms were able to chemisorbed as stable C—H bonds at these active sites. In fact, hydrocarbon groups such as $-CH$, $-CH_2$, or $-CH_3$

have been clarified by neutron diffraction measurements^{10,11} and IR absorption spectroscopy.¹² Although this product possesses high hydrogen capacity of 4–7 mass %, several essential disadvantages are also possessed for practical use. This product needs a high temperature of more than 700 °C to release the hydrogen and desorbs a large amount of hydrocarbons such as methane (CH_4) and ethane (C_2H_6) together with hydrogen. Furthermore, it is quite difficult to recharge this product with hydrogen under moderate conditions of pressure and temperature for the on-board application.

Recently, we have succeeded in improving the hydrogen desorption properties and the reversibility of the $C^{\text{nano}}H_x$ product by synthesizing the nanocomposites with alkali or alkaline-earth metal hydrides.¹³⁻¹⁶ Among these composites, the $C^{\text{nano}}H_x$ and LiH composite can typically store about 5.0 mass % of rechargeable hydrogen. Additionally, the amount of hydrocarbon desorption, which should be essentially desorbed from the $C^{\text{nano}}H_x$ product itself, is strongly suppressed in the case of this composite.¹⁴ It is considered that the polarized functional groups such as $-CH$, $-CH_2$, or $-CH_3$ at the edges or the defects in the $C^{\text{nano}}H_x$ product and the ionic crystal of LiH interact with each other, and then, both of them were destabilized. Therefore, hydrogen desorption from both components would be realized at lower

^{a)}Author to whom correspondence should be addressed. Tel./FAX: 81-82-424-5744. Electronic mail: tichi@hiroshima-u.ac.jp.

temperature than the decomposition temperature of each component by the interaction.^{13,14}

From these facts, it is noticed that the hydrogen absorption/desorption reactions of the Li—C—H system would be induced by the interaction between the polarized C—H groups in the $C^{\text{nano}}H_x$ and the LiH ionic crystal. Thus, it is considered that the hydrogenated state as well as dehydrogenated state should be characterized in order to understand the hydrogen absorption/desorption mechanism. In fact, it is difficult to investigate the states of this composite because the $C^{\text{nano}}H_x$ product possesses the characteristic hydrogenated state in the nanometer scale, which is quite different from standard hydride materials. In the case of a conventional x-ray diffraction (XRD) measurement, the scattering factor of x ray is roughly proportional to the atomic number. Thus, it is difficult to observe the correlations between hydrogen atoms and other atoms. On the other hand, neutron diffraction is a quite useful tool to investigate the location of hydrogen atoms because the coherent neutron scattering length possesses no systematic variation. Therefore, information about the bonding states of hydrogen atoms contained in the Li—C—H composite are able to be given by neutron diffraction measurements.

In this paper, thermal desorption analysis and structural investigation are carried out for the $C^{\text{nano}}H_x$ and LiH composites to characterize the hydrogen absorption/desorption properties. Furthermore, the correlations between the hydrogen atom and C or Li atom have been investigated by infrared absorption spectroscopy and neutron diffraction measurements for the as-synthesized, dehydrogenated, and rehydrogenated $C^{\text{nano}}H_x$ and LiH ($C^{\text{nano}}D_x$ and LiD) composites. On the basis of these results, the hydrogen absorption and desorption states of this composite are discussed.

II. EXPERIMENTAL PROCEDURES

A. Sample preparation

The $C^{\text{nano}}H_x$ and $C^{\text{nano}}D_x$ products were synthesized from graphite powder (99.999%, Stream Chemicals) by a rocking (shaking) ball-mill apparatus (Seiwa Giken Co. Ltd., RM-10) under hydrogen (H_2) and deuterium (D_2) atmospheres, respectively. 300 mg graphite and 20 ZrO_2 balls with 8 mm in diameter were put into a milling vessel with the inner volume of about 30 cm^3 made of Cr steel (Umetoku Co. Ltd., SKD-11). Then, ball milling was performed under a 1.0 MPa H_2 or D_2 for 80 h at room temperature. After the ball milling, the $C^{\text{nano}}H_x$ product was mechanically mixed with LiH (95%, Aldrich) by using a planetary (rotating) ball-mill apparatus (Fritsch, P7) for 2 h under a 1.0 MPa H_2 atmosphere to obtain close contact between both the components, in which a total of 300 mg of the $C^{\text{nano}}H_x$ product and LiH mixture were put into the Cr steel vessel with 20 ZrO_2 balls. The molar ratio of the C and LiH was chosen to be 2:1 based on previous study.¹³ In addition to this composite, the $C^{\text{nano}}D_x$ product was also mixed with LiD (98%, Aldrich) by ball milling under a 1.0 MPa argon (Ar) atmosphere in the same conditions as those of the $C^{\text{nano}}H_x$ and LiH composite, where these composites are named $C^{\text{nano}}H_x$ —LiH and $C^{\text{nano}}D_x$ —LiD. The dehydrogenating and

rehydrogenating treatments for these composites were performed at 350 °C for 8 h under high vacuum condition and 3 MPa H_2 , respectively. All the samples were handled in a glove box (Miwa MFG, MP-P60W) filled with purified Ar gas (>99.9999%) to avoid oxidation.

B. Experimental techniques

Thermal gas desorption properties of the as-prepared composites were examined by thermal desorption mass spectroscopy (TDMS) (Anelva, M-QA200TS) connected to thermogravimetry (TG) (Rigaku, TG8120). This equipment is installed inside the glove box especially to minimize the oxidation and the water adsorption on the samples. In the thermal analysis, high purity helium (He) gas (>99.9999%) was flowed as a carrier gas, and the heating rate was fixed at 5 °C/min. In the TDMS measurements for all the samples, some fragments related to genuine desorption gases such as H_2 , CH_4 , and C_2H_6 were monitored to assign desorbed gases. Phases in the composites were estimated by XRD measurement (Rigaku, RINT-2100, Cu $K\alpha$ radiation), where all the samples were covered by a polyimide sheet (Kapton®, Du Pont-Toray Co., Ltd.) in the glove box to avoid oxidation during the XRD measurement. The Fourier transform infrared (FTIR) spectroscopy (Spectrum One, Perkin-Elmer) was performed by using a diffuse reflection cell to examine IR active stretching modes in the composites. For the FTIR measurements, all the samples were diluted by potassium bromide (KBr) down to 10 mass %. The FTIR equipment is also installed inside a homemade glove box filled with purified argon gas to minimize oxidation further. The neutron diffraction measurements for the $C^{\text{nano}}D_x$ —LiD composites were carried out using a high intensity total scattering spectrometer (HIT-II) at the High Energy Accelerator Research Organization (KEK, Tsukuba, Japan). Then, each sample of about 1.0 g was put into a TiZr cell of 8.0 mm inner diameter with a 0.3 mm thick wall. Time-of-flight neutron scattering from a spallation neutron source is used to obtain detailed information on the short range atomic arrangement through a structure factor $S(Q)$ with higher Q up to 500 nm^{-1} . The $S(Q)$ was derived by applying various kinds of corrections to the background, absorption, and multiple scattering and normalizing with an incident neutron beam profile. Additionally, the radial distribution functions [RDF(r)] derived from Fourier transformation of $S(Q)$, where the densities of samples used for the calculation of RDF(r) were measured by gas pycnometer (micromeritics, Accupyc 1330) with He gas. The further details of experiment and analysis about the neutron diffraction measurements should be referred to the paper reported by Fukunaga *et al.*¹⁰ or Itoh *et al.*¹¹

III. RESULTS AND DISCUSSION

Figure 1(a) shows the TDMS and TG profiles of the $C^{\text{nano}}H_x$ —LiH composite, where mass numbers 2, 16, and 28 are assigned to H_2 , CH_4 , and C_2H_6 , respectively. Additionally, the intensities of CH_4 and C_2H_6 shown in Fig. 1 are enlarged ten times. The hydrogen desorption temperature is observed around 350 °C, which is much lower than the de-

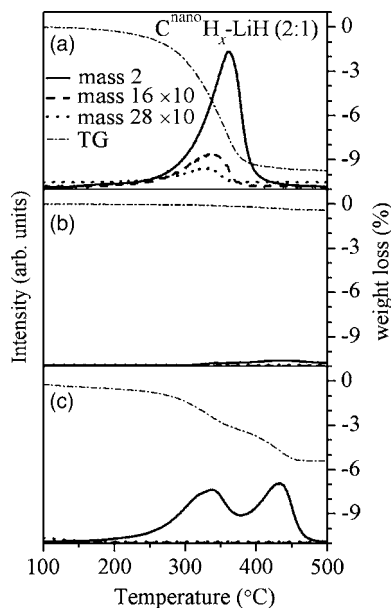


FIG. 1. TDMS and TG profiles (dash and dot line) of (a) the as-synthesized, (b) the dehydrogenated, and (c) the rehydrogenated $C^{\text{nano}}H_x$ —LiH composite, where mass numbers 2, 16, and 28 correspond to H_2 , CH_4 , and C_2H_6 , respectively.

composition temperatures of the $C^{\text{nano}}H_x$ product and LiH themselves. Although the $C^{\text{nano}}H_x$ product itself should desorb a large amount of hydrocarbons in a wide temperature range from 400 to 700 °C,^{6,14} it is noticed that this hydrocarbon desorption is strongly suppressed as shown in Fig. 1(a). These results indicate that the hydrogen atoms, which are included in this composite as the hydrocarbon group, could be desorbed as hydrogen instead of CH_4 and C_2H_6 due to interaction between the polarized functional groups in the $C^{\text{nano}}H_x$ product and LiH. With desorbing hydrogen by heating up to 500 °C, the TG profile of this composite [dash and dot line in Fig. 1(a)] reveals about 10.0 mass % weight loss, where this value includes the contribution of a small amount of the hydrocarbon desorption. The results of TDMS and TG measurements for the dehydrogenated $C^{\text{nano}}H_x$ —LiH composite are shown in Fig. 1(b). No clear peaks are observed and less than 1.0 mass % weight loss is revealed by heating up to 500 °C as shown in the TDMS and TG profiles, respectively, indicating that almost all hydrogen is desorbed due to the dehydrogenation at 350 °C for 8 h under high vacuum condition. As shown in Fig. 1(c), the hydrogen desorption profile of the rehydrogenated $C^{\text{nano}}H_x$ —LiH composite reveals a two-peak structure. Respective peaks corresponding to hydrogen desorption are located around 350 and 450 °C. Furthermore, it is noticed that only hydrogen is desorbed without any hydrocarbon emission, indicating that the hydrogenated state of the hydrogen recharged composite would be slightly different from that of the as-synthesized composite. The hydrogen desorption peak around 450 °C may be explained from kinetics because it is confirmed that these peaks almost disappeared by dehydrogenation at 350 °C. About 5.0 mass % weight loss is revealed due to only hydrogen desorption in the TG profile [dash and dot line in Fig. 1(c)]. Thus, it is expected that the $C^{\text{nano}}H_x$ —LiH composite can rechargeably store the hydrogen of 5.0 mass %.

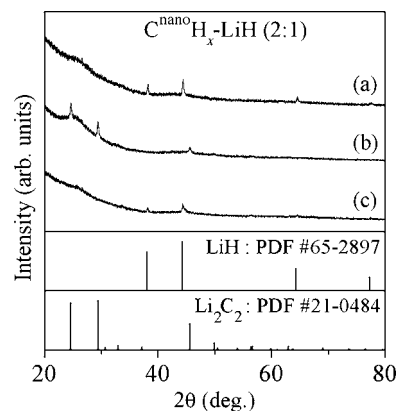


FIG. 2. XRD patterns of (a) the as-synthesized, (b) the dehydrogenated, and (c) the rehydrogenated $C^{\text{nano}}H_x$ —LiH composite at room temperature. The XRD patterns of LiH and Li_2C_2 are referred from the database (PDF No. 65-2897 and PDF No. 21-0484).

The XRD patterns of the $C^{\text{nano}}H_x$ —LiH composite after synthesizing, dehydrogenating, and rehydrogenating treatments are shown in Fig. 2. As reference, LiH (PDF No. 65-2897) and Li_2C_2 (PDF No. 21-0484) in the database are shown as well in Fig. 2. In the XRD pattern of the as-synthesized composite in Fig. 2(a), diffraction peaks corresponding to the LiH phase are observed. No other peaks related to the $C^{\text{nano}}H_x$ product appear, suggesting that the product in this composite should be the nanometer sized grains. After the dehydrogenation, it is clarified that the LiH phase disappears. On the other hand, new diffraction peaks assigned to Li_2C_2 appear as shown in Fig. 2(b). Furthermore, it is confirmed from the XRD pattern in Fig. 2(c) that the Li_2C_2 phase disappears and the LiH phase is recovered by the rehydrogenation at 350 °C under 3 MPa H_2 . However, it is clarified from the above results that at least LiH in the $C^{\text{nano}}H_x$ —LiH composite desorbs/absorbs hydrogen during the dehydrogenating/rehydrogenating treatments at 350 °C, the C—H correlations in the $C^{\text{nano}}H_x$ product were not able to be examined by the XRD measurements because the hydrogenated state of this product is quite different from those of crystalline metal hydrides.

In Fig. 3, the FTIR spectra of the $C^{\text{nano}}H_x$ product itself, the as-synthesized, dehydrogenated, and rehydrogenated $C^{\text{nano}}H_x$ —LiH composites, are shown. Some absorption

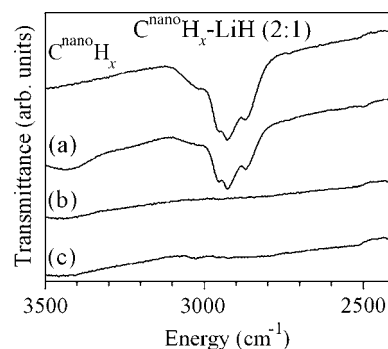


FIG. 3. FTIR spectra of (a) the as-synthesized, (b) the dehydrogenated, and (c) the rehydrogenated $C^{\text{nano}}H_x$ —LiH composite at room temperature, where the upper one is the spectrum of the $C^{\text{nano}}H_x$ product itself shown as a reference.

peaks are observed in the region from 2700 to 3200 cm^{-1} as shown in the FTIR spectrum of the $\text{C}^{\text{nano}}\text{H}_x$ product before mixing with LiH. With respect to these peaks, Ogita *et al.* reported that the origin of these peaks has been assigned to the stretching mode of $-\text{CH}_2$ and $-\text{CH}_3$ groups,¹² where any absorption peak corresponding to $-\text{CH}$ was not able to be observed by the FTIR measurement because of its weak signal. The FTIR spectrum of the as-synthesized composite in Fig. 3(a) reveals the peaks ascribed to the $-\text{CH}_2$ and $-\text{CH}_3$ groups at the same positions as those in the case of the $\text{C}^{\text{nano}}\text{H}_x$ product itself. This result indicates that the hydrogenated state as the C—H groups in the $\text{C}^{\text{nano}}\text{H}_x$ product is not changed by synthesizing the composite with LiH. In Fig. 3(b), it is clarified that these peaks disappear after heat treatment at 350 °C for 8 h, indicating that hydrogen atoms, chemisorbed as hydrocarbon groups, were desorbed at 350 °C thermodynamically. On the contrary, no peaks are observed by the FTIR measurement for the rehydrogenated composite as shown in Fig. 3(c). On the basis of these results, two possibilities would be thought to describe the rehydrogenated state of this composite. One is that the C—H bonding in this composite could not be detected by the FTIR measurement due to the small amount of those groups or the formation of only $-\text{CH}$ -type bonding. Another is that the C—H bonding could not be formed by the rehydrogenating treatment, which is performed at 350 °C under 3 MPa H_2 for 8 h. From the above results, it is clarified that hydrogen desorption from the as-synthesized composite at 350 °C, as shown in Fig. 1(a), includes the contribution of hydrogen contained as the polarized hydrocarbon groups in the $\text{C}^{\text{nano}}\text{H}_x$ product. On the other hand, it is expected that the hydrogenated state of the $\text{C}^{\text{nano}}\text{H}_x$ product after rehydrogenation is different from that in the as-synthesized composite.

It is clarified by TDMS, TG, XRD, and FTIR measurements that the $\text{C}^{\text{nano}}\text{D}_x$ —LiD composite reveals almost the same thermodynamic and structural properties as those of the $\text{C}^{\text{nano}}\text{H}_x$ —LiH composite. However, the results of the $\text{C}^{\text{nano}}\text{D}_x$ —LiD have not been shown in this paper to avoid repetition. The structure factors $[S(Q)]$ of the $\text{C}^{\text{nano}}\text{D}_x$ —LiD composite at each state obtained by neutron diffraction are shown in Fig. 4, where the $S(Q)$ of host graphite and LiD measured as reference are also included in the figure. As shown in Fig. 4(a), no peaks corresponding to graphite are observed in the spectrum of the as-synthesized composite although some observed peaks are assigned to LiD by comparing with the reference. Additionally, a large scattering intensity is observed in the small angle scattering region below 5.0 nm^{-1} in $S(Q)$. This result indicates that the graphite in the composite possesses the disordered states such as nanostructure or amorphous structure. Figure 4(b) shows $S(Q)$ of the dehydrogenated composite. Moreover, the main peaks of Li_2C_2 calculated from the powder XRD file of Li_2C_2 (PDF No. 21-0484) in the database are also shown in Fig. 4, where the intensity of each peak is assumed to be unity. The peaks corresponding to LiD completely disappear after the dehydrogenation. On the other hand, new peaks are observed, in which these are not consistent with the peaks corresponding to graphite shown as a reference in Fig. 4. Among them, the main peaks observed in $S(Q)$ are consistent with the peaks

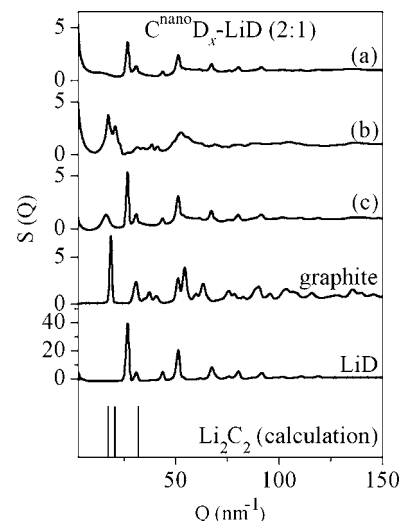


FIG. 4. Structure factors $[S(Q)]$ of (a) the as-synthesized, (b) the dehydrogenated, and (c) the rehydrogenated $\text{C}^{\text{nano}}\text{D}_x$ —LiD composite. The lower spectra are $S(Q)$ of host graphite, LiD, and main peaks of Li_2C_2 calculated from the database (PDF No. 21-0484) as reference.

calculated from the database of Li_2C_2 . Therefore, it is considered that the peaks observed after the dehydrogenation would be assigned to Li_2C_2 . As shown in Fig. 4(c), it is observed that the peaks corresponding to LiD are recovered after rehydrogenation. Moreover, a broad peak appears around 1.6 nm^{-1} in $S(Q)$, which would be assigned to the graphite (002), where it is noticed that the position of this peak is slightly shifted to lower Q compared to that of graphite shown as a reference. It is expected that this peak shift is induced by expansion of the graphite layers due to grain size of nanometer order. In addition to this result, the intensity in the small angle scattering region decreases compared to those of the as-synthesized and dehydrogenated composites. From these results, it is suggested that a small part of nanostructural graphite would be ordered by rehydrogenating treatment.

The RDF(r) obtained from $S(Q)$ of the as-synthesized $\text{C}^{\text{nano}}\text{D}_x$ —LiD composite is shown in Fig. 5. For the peaks observed within 0.25 nm, the correlations between atoms are estimated by fitting used Gaussian distribution functions. Additionally, some C—H groups, which are $-\text{CH}$, $-\text{CH}_2$, and $-\text{CH}_3$, are shown as models of hydrogen chemisorbed

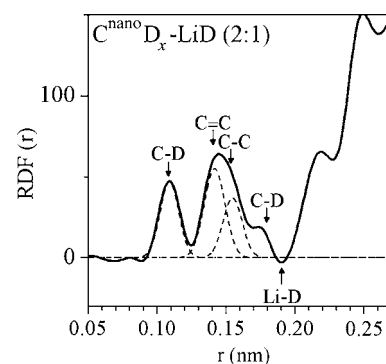


FIG. 5. Radial distribution function $\text{RDF}(r)$ of the as-synthesized $\text{C}^{\text{nano}}\text{D}_x$ —LiD composite. Dashed lines represent the fits using Gaussian distribution functions.

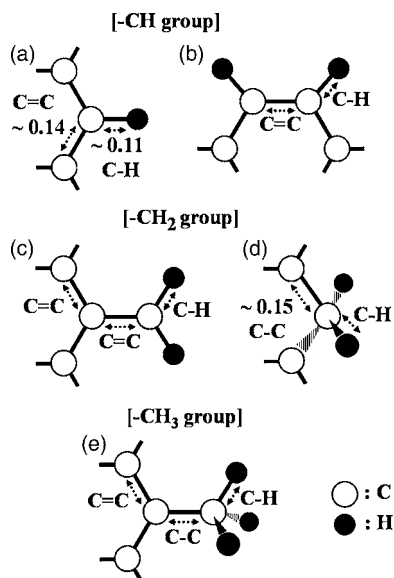


FIG. 6. Models of hydrogen chemisorbed state as $-\text{CH}$, $-\text{CH}_2$, and $-\text{CH}_3$ groups in the $\text{C}^{\text{nano}}\text{H}_x\text{-LiH}$ composite: $-\text{CH}$ group at (a) zigzag edges and (b) armchair edges, $-\text{CH}_2$ group with (c) sp^2 -hybridized carbon ($\text{C}=\text{C}$) and (d) sp^3 -hybridized carbon ($\text{C}-\text{C}$), and (e) $-\text{CH}_3$ group (where shown, the unit of length is in nm).

states in Fig. 6, where these models are built by geometric expectations and the previous studies. In this $\text{RDF}(r)$, two kinds of peaks related to $\text{C}-\text{C}$ correlation are observed at about 0.14 and 0.15 nm. The peak around 0.14 nm would originate in the bonding of sp^2 -hybridized carbon atoms ($\text{C}=\text{C}$) in the hexatomic ring of the graphite structure. With respect to another peak corresponding to the $\text{C}-\text{C}$ correlation, the bond length of 0.15 nm is close to that of sp^3 -hybridized carbon atoms ($\text{C}-\text{C}$) in crystalline diamond. Thus, it is expected that the fourfold bonding is generated due to the destruction of graphite structure by using ballmilling as shown in Figs. 6(d) and 6(e). It is also possible that some kinds of chained $\text{C}-\text{H}$ groups with the $\text{C}-\text{C}$ sp^3 bonding may exist at the edges in the nanostructural graphite. This result is consistent with the fact that the considerable amounts of the $-\text{CH}_2$ and $-\text{CH}_3$ groups are observed by the FTIR measurements as mentioned in the above section. Furthermore, the peaks corresponding to two kinds of the $\text{C}-\text{D}$ correlations are observed at about 0.11 and 0.18 nm, respectively, in this $\text{RDF}(r)$. The $\text{C}-\text{D}$ correlation observed around 0.11 nm is ascribed to the covalent bonds,¹⁰ suggesting that hydrogen atoms are chemisorbed at dangling bonds such as the edges or defects in graphene sheets produced by ball milling as models shown in Fig. 6. It is considered that the $\text{C}-\text{D}$ peak around 0.18 nm is assigned to the correlation between hydrogen atoms of the $\text{C}-\text{D}$ groups at the graphene edges and second neighbor carbon atoms ($\text{C}^{2\text{nd}}-\text{D}$). For these models of the $\text{C}-\text{H}$ group, the $\text{C}^{2\text{nd}}-\text{H}$ bond length is estimated by a geometrical calculation as follows. The $\text{C}^{2\text{nd}}-\text{H}$ bond length in the case of the covalent bond at zigzag edges in the ab plane as model (a) in Fig. 6 is estimated as about 0.22 nm, which is longer than 0.18 nm. On the other hand, it is possible that the $\text{C}^{2\text{nd}}-\text{H}$ bond length of other models is estimated to be around 0.18 nm if the atoms form a suitable $\text{C}-\text{C}-\text{H}$ bond angle.

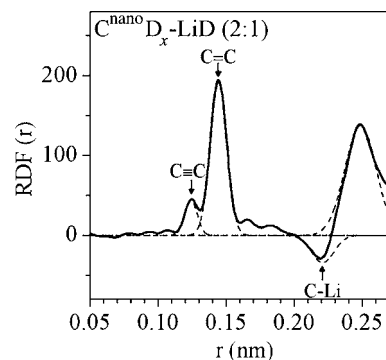


FIG. 7. Radial distribution function $\text{RDF}(r)$ of the dehydrogenated $\text{C}^{\text{nano}}\text{D}_x\text{-LiD}$ composite. Dashed lines represent the fits using Gaussian distribution functions.

The bond length of 0.18 nm might be realized in a situation when the hydrogen atom in models (a)–(c) exists out of the ab plane, where the $\text{C}-\text{C}-\text{H}$ bond angle should be around 91° . In addition to the above $\text{C}-\text{C}$ and $\text{C}-\text{D}$ correlations, it is noticed that the negative correlation is revealed at about 0.19 nm. In fact, this peak is not clear because the negative peak overlaps with the positive correlation around 0.18 nm, so that it is quite difficult to perform the fitting by Gaussian distribution functions for both peaks. Here, it is clarified from $\text{RDF}(r)$ obtained by neutron diffraction for LiD itself that the $\text{Li}-\text{D}$ correlation is revealed as a negative peak, where the $\text{RDF}(r)$ of LiD is omitted in this paper because a coherent scattering length of Li atom is the only negative value among those of the atoms included in this composite. Furthermore, the result of the XRD measurements and $S(Q)$ of the $\text{C}^{\text{nano}}\text{D}_x\text{-LiD}$ composites demonstrates the existence of LiD. From these experimental facts, the negative correlation is assigned to the $\text{Li}-\text{D}$ bond. Figure 7 shows the $\text{RDF}(r)$ of the dehydrogenated $\text{C}^{\text{nano}}\text{D}_x\text{-LiD}$ composite. In the $\text{RDF}(r)$, three kinds of characteristic peaks are revealed at about 0.12, 0.14, and 0.22 nm. The peak around 0.14 nm is assigned to the $\text{C}=\text{C}$ correlation of sp^2 bonding in nanostructural graphite, which is sharper than that of the as-synthesized composite. The positive peak around 0.12 nm and the negative peak around 0.22 nm are ascribed to the $\text{C}-\text{C}$ and $\text{C}-\text{Li}$ correlations in Li_2C_2 , respectively. The crystal structure of Li_2C_2 has been investigated and reported before.^{17,18} Among those studies, Ruschewitz and Pottgen reported on the crystal structure Li_2C_2 obtained by XRD measurements.¹⁸ In that paper, it is determined that the bond length of the $\text{C}-\text{C}$ correlation in Li_2C_2 is about 0.123 nm. This $\text{C}-\text{C}$ bond would be the typical $\text{C}-\text{C}$ triple bond ($\text{C}\equiv\text{C}$) of sp hybridization, where this bond length is close to that of 0.120 nm in acetylene. Thus, the $\text{C}-\text{C}$ correlation around 0.12 nm is assigned to the $\text{C}-\text{C}$ triple bond in Li_2C_2 . The obvious negative peak around 0.22 nm should be ascribed in a correlation related to Li atom. By comparing with the $\text{RDF}(r)$ of the as-synthesized composite, this bond length is longer than that of 0.19 nm in the case of the $\text{Li}-\text{D}$ correlation. It is confirmed from XRD pattern and $S(Q)$ that the LiD phase disappeared after dehydrogenation. From these experimental facts, it can be explained that the origin of the peak around 0.22 nm is caused by the $\text{C}-\text{Li}$

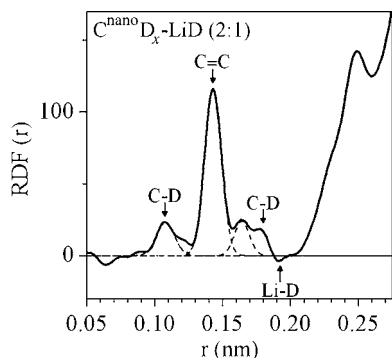


FIG. 8. Radial distribution function $RDF(r)$ of the rehydrogenated $C^{\text{nano}}D_x$ -LiD composite. Dashed lines represent the fits using Gaussian distribution functions.

correlation in Li_2C_2 . The $RDF(r)$ of the rehydrogenated $C^{\text{nano}}D_x$ -LiD composite is shown in Fig. 8. The peaks assigned to Li_2C_2 disappear, and then the Li—D correlation assigned to the LiD phase is recovered at about 0.19 nm, where this phenomenon has been clarified by the XRD measurement already. The peak ascribed to the $C=C$ sp^2 bonding is also observed around 0.14 nm. On the other hand, the peak at 0.15 nm of the as-synthesized composite is not revealed in the $RDF(r)$ profile of the rehydrogenated composite. Considering these results, it is expected that the amount of sp^3 -hybridized carbon atoms decrease due to the structural order by the hydrogen desorption and absorption treatments, where this result is consistent with the behavior in the small angle scattering region in $S(Q)$. It is noticed that the peaks corresponding to the C—D correlation are obviously recovered around 0.11 and 0.18 nm as shown in Fig. 8 although the C—H bonding is difficult to be observed by the FTIR measurement. Therefore, it is considered that the only hydrogen desorption from the rehydrogenated composite is realized by the interaction between the polarized C—H bonding at the dangling bonds of nanostructural graphite and LiH. The intensity of the peak around 0.11 nm is slightly weak in comparison to that of the as-synthesized composite, indicating that the amount of chemisorbed hydrogen at the dangling bonds is smaller than that in the as-synthesized composite. In addition, a new peak is observed at about 0.16 nm, which is longer than that of the C—C bonds of ~ 0.15 nm or shorter than that of $C^{2\text{nd}}\text{—H}$ bond of ~ 0.18 nm. Thus, it seems likely that the origin of this peak might be a new C—D correlation, which is different from the $C^{2\text{nd}}\text{—D}$ correlation revealed around 0.18 nm, as one of the possibilities. From the above results of the neutron diffraction measurements, it is clarified that not only Li but also nanostructural carbon (C^{nano}) in this composite can be recharged with hydrogen by the rehydrogenating treatment at 350 °C under 3 MPa of hydrogen pressure.

IV. CONCLUSION

In this work, various kinds of measurements are carried out to characterize the hydrogen absorbed and desorbed states of the $C^{\text{nano}}H_x$ -LiH composite. In particular, the neutron diffraction measurement has provided some important

information about the change in the C—H correlations in this composite with hydrogen absorption and desorption.

In the as-synthesized $C^{\text{nano}}D_x$ -LiD composite, some C—D and Li—D correlations are observed by the neutron diffraction measurement. Among them, the characteristic peaks are ascribed to the C—D covalent bond, the C—C sp^3 -hybridized bond, and the C—D correlation between the deuterium atoms and second nearest carbons ($C^{2\text{nd}}\text{—D}$), which are located around 0.11, 0.15, and 0.18 nm in the $RDF(r)$, respectively. From these results, it is considered that hydrogen atoms are chemisorbed as the polarized C—H bonds such as the —CH, —CH₂, and —CH₃ groups at the dangling bonds, which exist at the edges or the defects generated due to the destruction of graphite structure with ball milling. Actually, the hydrogen atoms contained in both the components are desorbed as hydrogen gas by the interaction between such polarized C—H groups and LiH. On the other hand, it seems likely that a part of the C—H groups with the sp^3 -hybridized carbon atoms could not react with LiH. Then, these C—H groups are desorbed as quite a small amount of hydrocarbons. Therefore, it is considered that the hydrocarbon desorption would originate in disordering in the edge or defect states in nanostructural graphite.

With the hydrogen desorption reaction, it is clarified by x-ray and neutron diffraction measurements that the LiH phase and the C—D correlations disappear and Li_2C_2 is formed.

After rehydrogenation, the results of XRD measurements and structure factors $S(Q)$ indicate that the LiH (LiD) phase is recovered. Furthermore, it is clarified by neutron diffraction measurements that hydrogen atoms are recharged as the C—D groups at the dangling bonds in the nanostructural graphite. Additionally, the C—C sp^3 -hybridized bonding is not observed after rehydrogenation, indicating that the amount of the C—H groups in this composite would decrease by ordering the edge or the defect states in nanostructural graphite with dehydrogenating/rehydrogenating reactions at 350 °C. Therefore, it is considered that the rehydrogenated composite can desorb only hydrogen without hydrocarbon emission.

ACKNOWLEDGMENT

This work was supported by the project “Development for Safe Utilization and Infrastructure of Hydrogen Industrial Technology” of the New Energy and Industrial Technology Development Organization (NEDO) and Research Fellowships of the Japan Society for the Promotion of Science for Young Scientists (JSPS). The authors gratefully acknowledge Dr. Isobe and Dr. Paik for useful discussion and valuable help in this work.

¹L. Schlapbach and A. Züttel, *Nature (London)* **414**, 353 (2001).

²W. Grochala and P. P. Edwards, *Chem. Rev. (Washington, D.C.)* **104**, 1283 (2004).

³F. Schüth, B. Bogdanović, and M. Felderhoff, *Chem. Commun. (Cambridge)* **2004**, 2243.

⁴A. C. Dillon, K. M. Jones, T. A. Bekkedahl, C. H. Kiang, D. S. Bethune, and M. J. Heben, *Nature (London)* **386**, 377 (1997).

⁵S. Orimo, G. Majer, T. Fukunaga, A. Züttel, L. Schlapbach, and H. Fujii, *Appl. Phys. Lett.* **75**, 3093 (1999).

- ⁶S. Orimo, T. Matsushima, H. Fujii, T. Fukunaga, and G. Majer, *J. Appl. Phys.* **90**, 1545 (2001).
- ⁷D. M. Chen, T. Ichikawa, H. Fujii, N. Ogita, M. Udagawa, Y. Kitano, and E. Tanabe, *J. Alloys Compd.* **354**, L5 (2003).
- ⁸S. Isobe, T. Ichikawa, J. I. Gottwald, E. Gomibuchi, and H. Fujii, *J. Phys. Chem. Solids* **65**, 535 (2004).
- ⁹T. Ichikawa, D. M. Chen, S. Isobe, E. Gomibuchi, and H. Fujii, *Mater. Sci. Eng., B* **108**, 138 (2004).
- ¹⁰T. Fukunaga, K. Itoh, S. Orimo, and K. Aoki, *Mater. Sci. Eng., B* **108**, 105 (2004).
- ¹¹K. Itoh, Y. Miyahara, S. Orimo, H. Fujii, T. Kamiyama, and T. Fukunaga, *J. Alloys Compd.* **356**, 608 (2003).
- ¹²N. Ogita, K. Yamamoto, C. Hayashi, T. Matsushima, S. Orimo, T. Ichikawa, H. Fujii, and M. Udagawa, *J. Phys. Soc. Jpn.* **73**, 553 (2004).
- ¹³T. Ichikawa, H. Fujii, S. Isobe, and K. Nabeta, *Appl. Phys. Lett.* **86**, 241914 (2005).
- ¹⁴T. Ichikawa, S. Isobe, and H. Fujii, *Mater. Trans.* **46**, 1757 (2005).
- ¹⁵H. Miyaoka, T. Ichikawa, S. Isobe, and H. Fujii, *Physica B* **383**, 51 (2006).
- ¹⁶H. Miyaoka, T. Ichikawa, and H. Fujii, *J. Alloys Compd.* **432**, 303 (2007).
- ¹⁷R. Juza, V. Wehle, and H. U. Schuster, *Z. Anorg. Allg. Chem.* **352**, 252 (1967).
- ¹⁸U. Ruschewitz and R. Pottgen, *Z. Anorg. Allg. Chem.* **625**, 1599 (1999).